830 Å.[14] Apparently Maki's analysis in its present form does not apply to our films.

The observed dependence of the transport entropy on film thickness does seem to corroborate our earlier data. If indeed Pb at 4.2 K behaves like a type-II superconductor for films thinner than 1.5 μm, then it is not surprising that S_φ/φ is reduced. This behavior is likely attributable to the increased interactions between the closely spaced vortices.[7]

IV. CONCLUSIONS

The present experiments on the Ettingshausen effect confirm our earlier results from Nernst effect measurements that the transport entropy per unit length and per unit flux, S_φ/φ, decreases with decreasing film thickness below a critical thickness value. This behavior can be understood through the increasing vortex interaction in very thin type-I films. For the 3.16-μm film, sufficiently below H_c, S_φ/φ is very close to the value calculated from simple thermodynamic arguments, whereas for the 0.75-μm film it is considerably reduced.

* Based on work performed under the auspices of the U.S. Atomic Energy Commission.

[1] Gordon Lasher, Phys. Rev. **154,** 345 (1967).
[2] Kazumi Maki, Ann. Phys. (N.Y.) **34,** 363 (1965).
[3] M. Tinkham, Phys. Rev. **129,** 2413 (1963).
[4] G. D. Cody and R. E. Miller, Phys. Rev. **173,** 494 (1968).
[5] G. D. Cody and R. E. Miller, Phys. Rev. **173,** 481 (1968).
[6] J. A. Cape, Phys. Rev. **166,** 432 (1968).
[7] R. P. Huebener and A. Seher, Phys. Rev. **181,** 710 (1969); R. P. Huebener and V. A. Rowe, Solid State Commun. **7,** 1763 (1969); V. A. Rowe and R. P. Huebener, Phys. Rev. **185,** 666 (1969).
[8] P. R. Solomon and F. A. Otter, Jr., Phys. Rev. **164,** 608 (1967); P. R. Soloman, *ibid.* **179,** 475 (1969). Note that the correct spelling is Ettingshausen, and not Ettinghausen as appears in much of the literature.
[9] Source: Division Lead Company, Summit, Ill.
[10] Source: Emerson & Cuming, Inc., Canton, Mass.
[11] K. Mendelssohn and J. L. Olsen, Proc. Phys. Soc. (London) **A63,** 2 (1950); Phys. Rev. **80,** 859 (1950); N. V. Zavaritskii, Zh. Eksperim. i Teor. Fiz. **38,** 1673 (1960) [Soviet Phys. JETP **11,** 1207 (1960)]; K. Mendelssohn and C. A. Shiffman, Proc. Roy. Soc. (London) **A255,** 199 (1960).
[12] John R. Clem, Phys. Rev. **176,** 531 (1968); Phys. Rev. Letters **20,** 735 (1968).
[13] Kazumi Maki, Progr. Theoret. Phys. (Kyoto) **42,** 448 (1969).
[14] J. Bardeen and J. R. Schrieffer, *Progress in Low Temperature Physics,* edited by C. J. Gorter (North-Holland, Amsterdam, 1961), Vol. III, p. 243.

PHYSICAL REVIEW B VOLUME 2, NUMBER 11 1 DECEMBER 1970

rf-Induced Effects in Superconducting Tunnel Junctions*

C. A. HAMILTON AND SIDNEY SHAPIRO
Department of Electrical Engineering, University of Rochester, Rochester, New York 14627

(Received 15 July 1970)

Arguments are presented to resolve experimental discrepancies with the theory of photon-assisted tunneling. A standing-wave model is suggested as a more realistic picture of the rf fields in a thin-film tunnel junction. By including the effects of this model in the theories of Tien and Gordon and of Werthamer, we obtain qualitative agreement with data on both the Josephson effects and the photon-assisted tunneling effects in the same junction. In an experiment with a junction sufficiently small to maintain a uniform rf field, we find excellent agreement with the unmodified theory. The low-frequency equivalence of the photon-assisted tunneling phenomenon and classical rf detection is also pointed out and used to demonstrate that the magnitude of the rf voltage appears correctly in the theory. We conclude that the Werthamer theory of rf-induced effects in superconducting tunnel junctions is on very firm experimental ground.

I. INTRODUCTION

It is well known that the current-voltage (I-V) characteristic of a superconducting tunnel junction is modified in the presence of an applied rf field. Constant-voltage steps arise from the interaction of the rf field with the ac Josephson current. In addition, the background curve is modified by a series of rounded steps caused by rf effects on the quasiparticle tunnel current. In this paper we present arguments to explain experimental discrepancies with the theory of the quasiparticle effects. Werthamer[1] has shown that the ac Josephson currents and the quasiparticle tunnel currents are intimately related in theory. We demonstrate this relationship experimentally and thus support our conclusions with data on both of these effects.

Observation of the quasiparticle steps, often called photon-assisted tunneling steps, was first reported by Dayem and Martin.[2] These steps in the I-V curve are spaced at voltage intervals of hf/e up and down from the superconducting energy-gap voltage and may be thought of as arising from multiphoton emission and absorption processes. Each step is a sharp increase in current and has the same shape as the current increase at the energy-gap voltage $2\Delta/e$ in the undisturbed I-V curve. This phenomenon was first explained quantitatively by Tien and Gordon.[3] Their result is based on the assumption that the effect of the microwave field is a sinusoidal modulation of the bias voltage across the junction. Their analysis correctly predicts the voltages at which steps should appear and indicates that the

current magnitude of each step should vary as the square of a Bessel function (J_n^2) whose argument is proportional to the rf voltage. A detailed analysis by Werthamer[1] has verified the Tien-Gordon result and shown that the rf-voltage dependence of the ac Josephson steps and the photon-assisted tunneling steps arises from the same term in the microscopic theory (namely, the time-dependent phase difference across the junction). Since the predictions for the rf-voltage dependence of the ac Josephson effect have been verified in point-contact junctions,[4] as well as in thin-film junctions at low frequencies,[5] we expect the theory also to be correct in the case of photon-assisted tunneling steps.

Two important discrepancies have been reported between experimental results and this theory. First, the observed rf-voltage dependence of the steps does not follow the J_n^2 form; second, the predicted value of rf voltage required to observe the effect is about two orders of magnitude greater than the estimated rf voltage in the experiment.[3,6,7]

Using tin-oxide-tin thin-film junctions, we have studied the rf-voltage dependence of both the Josephson and quasiparticle steps. These steps have been observed with high resolution by using a combination of a low temperature, $T=1.3$°K, a high frequency, $f=70$ to 80 GHz, and derivative techniques in which junction resistance or conductance is plotted versus voltage or current. This high resolution enabled us to observe and measure the rf-voltage dependence of as many as ± 13 quasiparticle steps in a single sequence. One sequence of steps associated with the positive gap voltage is thus seen to extend through the origin and overlap the steps arising from the negative gap voltage. These experiments have shown that with increasing rf voltage the quasiparticle steps appear in order, each step rising sharply to a maximum and then decreasing gradually. This result is in agreement with the general form of the rf-voltage dependence reported previously but clearly in contrast to the predicted J_n^2 dependence, since there are no points in the experimental data where the step magnitudes go through zeros.

We propose that this problem can be resolved by including the effects of a standing-wave rf-voltage variation across the tunnel junction. We show that this assumption modifies the predicted Bessel-function rf-voltage dependence of both the ac Josephson steps and the quasiparticle steps in a way which is consistent with experimental observations. We have also performed experiments on junctions too small to have an rf-voltage variation and found excellent agreement with the *unmodified* theory.

The second point to be resolved concerns the magnitude of rf voltage across the junction required to observe the quasiparticle steps. Previous estimates of this voltage have been made by integrating the undisturbed electric field in the vicinity of the junction over a distance equal to the oxide barrier thickness.[3,6,8] Such a calculation ignores the very large perturbation on the electric field caused by the presence of the junction. In fact, the resonantlike structure indicated by our standing-wave model suggests that the field in the junction may be very much larger than the external field.

Further light is shed on this question by examining the behavior of the quasiparticle steps at low frequencies. Such experiments[8] have not shown resolved steps but instead a gradual smoothing of the I-V curve when rf power is applied. This kind of behavior is commonly associated with classical rf detection.[9] We show that the Tien-Gordon expression reduces exactly to classical rf detection at low frequencies. This verification of the Tien-Gordon result in the low-frequency limit strengthens our confidence in the theory and demonstrates that the magnitude of $V_{\rm rf}$ required by the theory must be correct at low frequencies. To demonstrate this point we performed an experiment at a frequency sufficiently low that $V_{\rm rf}$ could be measured directly. As expected, our data using a measured $V_{\rm rf}$ follow the theory exactly. We thus conclude that the magnitude of $V_{\rm rf}$ appears correctly in the theory and that previous reports to the contrary are the result of the improper methods used to estimate $V_{\rm rf}$.

In Sec. II we describe our experimental procedures. In Sec. III we present the standing-wave model and its experimental justification. The low-frequency equivalence of the Tien-Gordon expression and classical rf detection is demonstrated and discussed in Sec. IV. In Sec. V we summarize our conclusions and discuss them with respect to other contributions in the field.

II. EXPERIMENTAL PROCEDURES

All of our experiments used tin-oxide-tin thin-film junctions. The samples were prepared in a conventional diffusion-pump evaporator using a liquid-nitrogen baffle. Most test runs employed two cross-type junctions, about 0.1 mm square made on a $0.25\times0.50\times0.010$-in.-thick substrate.

Before evaporation the substrate was cleaned in a glow discharge for about 15 min. In order to make four separate evaporations without opening the system to the atmosphere, the substrate was mounted directly under a rotating mask. Each 20° segment of the mask contained one of the four patterns used to make the completed sample. These were (i) two parallel strips of tin with (ii) thick Cerroseal (65% indium, 35% tin) connection pads and (iii) a crossing Z-shaped strip of tin with (iv) its connection pads. A single tungsten boat was used as a source for all evaporations. Film thickness (typically 700 Å) was controlled by loading the boat with a measured quantity of metal and evaporating to completion. Evaporation time was 10–15 sec at a maximum pressure of 6×10^{-6} Torr. Substrate temperature during evaporation was -20°C. This low temperature substantially reduced secondary evaporation from the substrate surface, thus improving continuity and edge sharpness. The oxide barrier was formed by warm-

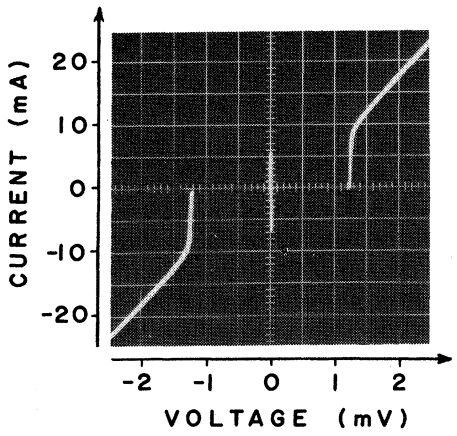

FIG. 1. Oscilloscope trace of the I-V curve for a typical 0.1-Ω superconducting tin-oxide-tin junction.

ing the substrate to 20°C and exposing the tin film to a glow discharge in pure dry oxygen at 0.12-Torr pressure for about 40 sec. Oxidation for longer times did not significantly increase the junction resistance and seemed, in fact, to cause microshorts in the barrier. Total sample-preparation time was about 1 h.

I-V curves were measured using the conventional four-wire connection with a constant-current drive. Dynamic resistance (dV/dI) measurements were made by inserting a small ac constant-current signal onto the dc-bias current. A lock-in amplifier tuned to the ac frequency was used to detect the corresponding ac signal in the junction voltage. This signal was directly proportional to dV/dI. Conductance (dI/dV) was similarly measured by using a low-impedance (constant-voltage) drive and detecting the ac component of junction current.

Typical junction resistance was 0.1 Ω measured at 1.3°K. It is important to note that in spite of the four-wire measuring system, film resistance over the area of the junction will cause incorrect measurements of tunneling resistance (sometimes even negative) unless the films are entirely superconducting.[10]

The substrate was mounted in a slot across an M-band (0.148×0.074 in.) waveguide such that the E field (for the TE_{10} mode) was perpendicular to the plane of the junctions. The waveguide was terminated with an adjustable short so that the field pattern in the vicinity of the junction could be adjusted to maximize coupling. A precision attenuator provided a measure of the relative power level. Reflex klystrons at 20, 70, and 80 GHz were used as rf sources. For the experiments at 20 GHz a similar rig was employed with the junction mounted across X-band (0.9×0.4 in.) waveguide.

The substrate and its microwave mounting were immersed directly in the liquid helium. All of our data were taken at a temperature of about 1.3°K, which could be obtained by pumping on the helium bath with a mechanical pump. In this temperature range we did not find our results to be particularly temperature sensitive, although resolution generally improved with decreasing temperature.

A magnetic field could be applied parallel to the plane of the junction by a coil outside the Dewar. A small field was used to study the junction self-resonant structure (Fiske modes). A somewhat larger field (20 G) was often used to quench the ac Josephson effects when it was desirable to study only the effects of the quasiparticle tunnel current.

An oscilloscope trace of a typical I-V curve is shown in Fig. 1. Junction resistance R is measured from the slope of the curve at voltages greater than the gap voltage $2\Delta/e$. The lack of any significant current at lower voltages is an indication of the absence of microshorts or other nontunneling processes. The dc Josephson current (spike at zero voltage) is about 80% of the maximum theoretical value of $\pi\Delta/2eR$. The effect of the constant-current drive is also clear from the switching points at $V=0$ and at the ends of the dc Josephson current. Further experimental detail is given when our data are presented.

III. STANDING-WAVE MODEL

A. Experiment and Theory Compared

The photon-assisted tunneling steps were first explained qualitatively by Dayem and Martin.[2] In their model, an electron in one superconductor with an energy hf less than the lowest available state in the other superconductor can absorb a photon from the microwave field and tunnel through the barrier. This new current-carrying process begins at a threshold energy equal to the gap energy less the energy of one photon and consequently gives rise to a step in current at the corresponding voltage. The tunneling current at this threshold voltage is greatly enhanced by the peak in the density of states at the energy-gap edge. The series of steps at $2\Delta/e\pm nhf/e$ is similarly explained in terms of multiphoton emission or absorption processes.

The quantitative calculation made by Tien and Gordon[3] assumed that the voltage across the junction in the presence of rf could be written

$$V=V_{dc}+V_{rf}\cos 2\pi ft. \quad (1)$$

This time-dependent potential is used as a modification of the Hamiltonian for states on one side of the junction. Their analysis leads to a new effective density of states which is a function of V_{rf}. The resulting tunnel current is

$$I_{dc}(V_{dc})=\sum_{n=-\infty}^{\infty} J_n^2(eV_{rf}/hf)I_0(V_{dc}+nhf/e), \quad (2)$$

where $I_0(V_{dc})$ is the usual tunnel characteristic for a superconducting diode and J_n is the Bessel function of order n.

As a result of the peak in the superconducting density of states at the energy-gap edge, $I_0(V_{dc})$ has a large step in current at the gap voltage $2\Delta/e$. The width of this step for a typical tin-oxide-tin junction is about 60 μV. We therefore define high frequency to be such that $hf/e>60$ μV. Thus for "high" frequencies (15 GHz and up), Eq. (2) predicts a series of steps in the I-V curve spaced at voltage intervals of hf/e up and down from the gap voltage. Each of these steps results from the addition of a new current-carrying channel and is a reflection of the step at $V=2\Delta/e$ in the undisturbed I-V curve, $I_0(V_{dc})$. Equation (2) indicates that the height of these steps in current should vary as $J_n^2(eV_{rf}/hf)$.

Using the assumption of Eq. (1), the detailed microscopic theory of Werthamer[1] also yields an expression for the dc junction current in the presence of an applied rf field. His analysis includes both the Josephson effects and the quasiparticle effects. In the case of the quasiparticle effects the result is identical to Eq. (2). Since both Werthamer and Tien and Gordon based their calculations on an oscillating potential in only one superconductor, their procedure appears to be asymmetric. However, Büttner and Gerlach[11] have recently shown that the same result may be obtained from a symmetrical treatment of the rf voltage.

Ignoring the frequency-dependent terms, which are not important in our experiment, Werthamer's result for the ac Josephson steps is given by

$$I_{dc}(V_{dc})=I_{dc}(0)\sum_{n=-\infty}^{\infty}|J_n(2eV_{rf}/hf)|\,\delta(V_{dc}-nhf/2e), \tag{3}$$

where $I_{dc}(0)$ is the dc Josephson current and δ is the usual δ function. This equation describes the spacing and rf-voltage dependence of the well-known ac Josephson steps first observed by Shapiro.[12] It is important to our development because observation of the ac Josephson steps provides another measure of V_{rf}.

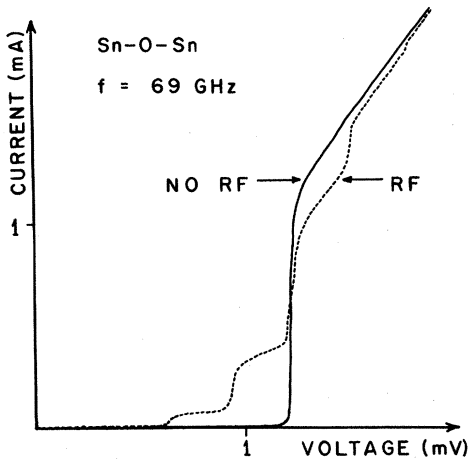

FIG. 2. X-Y recorder plot of a tunnel-junction I-V curve with and without applied radiation at 69 GHz.

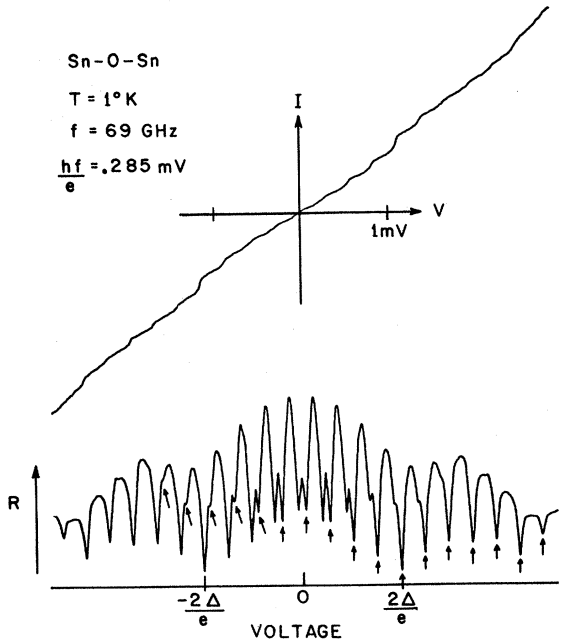

FIG. 3. I-V curve and its derivative $R=dV/dI$ versus V for a junction exposed to 69-GHz radiation at a high power level. The arrows point to the resistance minima of steps associated with the positive gap voltage.

We can now turn our attention back to the photon-assisted tunneling steps. Figure 2 shows a typical I-V curve for a tin-oxide-tin junction with and without an applied rf field at 69 GHz ($hf/e=0.285$ mV). A magnetic field has been used to suppress the Josephson current and the associated rf-induced steps. In the presence of rf, two photon-assisted tunneling steps are visible above and below the gap voltage. Figure 3 is a similar I-V curve and its derivative at a higher rf power level. The two overlapping series of steps associated with the positive and negative gap voltage are clearly visible in the derivative curve.

Several methods have been used to measure the height in current of the quasiparticle steps as a function of rf voltage. If the steps are sharply defined, their height may be measured by taking the vertical distance at the step voltage between tangent lines to the I-V curve just above and below the step. For poorly resolved steps the height may be measured as the width of the resistance dip in a plot of dV/dI versus I. A third method was used for experiments at 20 GHz, where we estimated step heights from the magnitude of the conductance peaks in a plot of dI/dV versus V. All values of step height are normalized to the height of the step at the gap voltage ($n=0$) with $V_{rf}=0$. The relative value of V_{rf} is computed from the precision attenuator reading (in dB) and all values are multi-

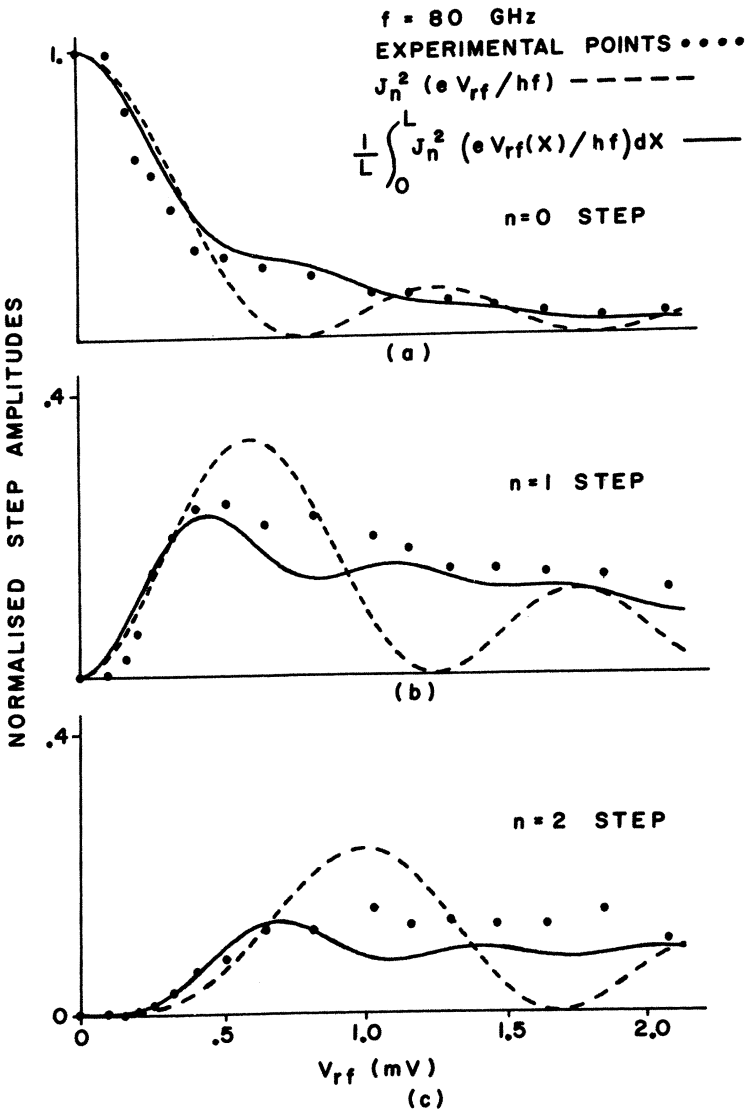

FIG. 4. Quasiparticle-step amplitudes for the $n=0$, 1, and 2 steps as a function of V_{rf}.

plied by a single constant C to obtain a best fit to the theory, i.e., $V_{rf}=C\times 10^{-(dB/20)}$.

In Figs. 4(a), 4(b), and 4(c) the points indicate current-step magnitudes measured from the I-V curves for the $n=0$, 1, and 2 steps, respectively, in a 0.1-mm-square junction exposed to 80-GHz radiation. The experimental behavior is clearly contrary to the squared Bessel-function V_{rf} dependence of Eq. (2) (shown as the dashed line) because there are no points in the experimental data where the step currents go through zeros.

B. Standing-Wave Model

We propose that the explanation for this lies in the fact that there is a spatial variation of the rf voltage across the junction. Since the penetration depth in the films ($\lambda\simeq 500$ Å) is very much greater than the barrier thickness ($l=10$–20 Å), the electromagnetic wave in the junction exists mostly in the metal. The consequent inductive loading leads to a drastic reduction in the wave velocity given by[13]

$$\bar{c}=c[l/\epsilon(2\lambda+l)]^{1/2}, \tag{4}$$

where ϵ is the effective dielectric constant in the oxide. Using $\epsilon=5$, Eq. (4) leads to a wavelength of about 0.17 mm at a frequency of 80 GHz. Thus, as indicated at the top of Fig. 5, even though our junctions are much smaller than a guide wavelength ($\simeq 4$ mm), they will have a spatial variation of V_{rf} which is about one-half wavelength long.

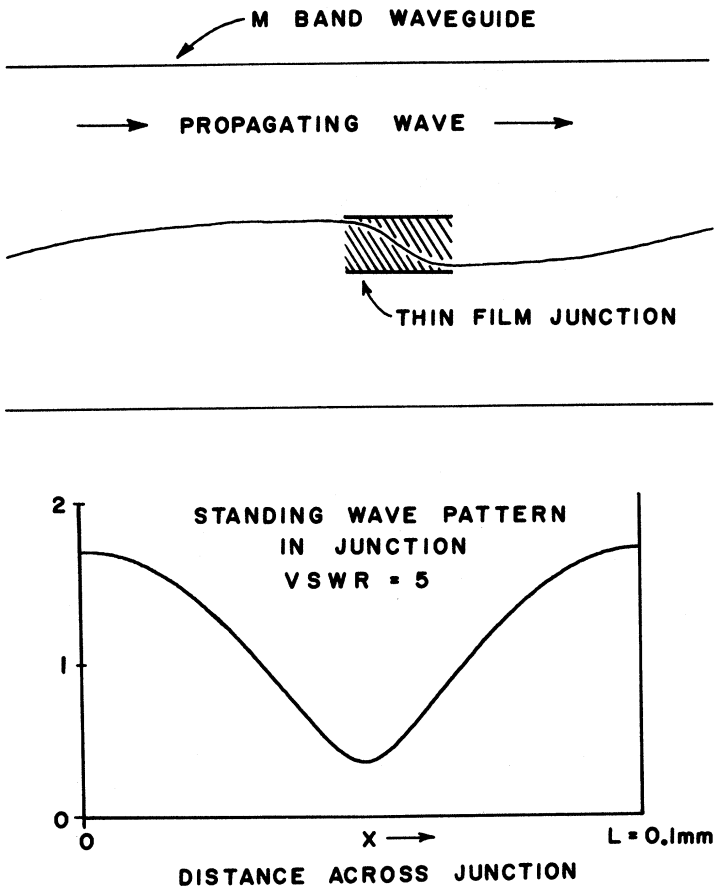

FIG. 5. Schematic representation of the reduced junction wavelength and the resulting standing-wave pattern.

This conclusion is supported by observation of the junction self-resonant modes, frequently called Fiske modes.[14] In the presence of a small magnetic field, these modes are excited by the ac Josephson current and appear as constant-voltage steps in the I-V curve. In our 0.1-mm-square junctions these modes are spaced at 50–100 GHz, indicating a half-period field variation in this frequency range.

As a result of the large impedance mismatch between the junction and the surrounding structure, we expect a large reflection at the boundaries, thus giving rise to standing waves. Although he did not analyze this case, Werthamer has also pointed out the validity of the standing-wave model as the correct picture of rf fields within thin-film junctions. The standing-wave pattern at the bottom of Fig. 5 indicates this model of the spatial variation of rf voltage in our junctions. It is a one-dimensional standing-wave pattern one-half wavelength long with a fairly high voltage standing-wave ratio (VSWR). We choose this simplified model for what is in reality a complicated field problem, since it includes what is physically essential.

Using this model, the current can be calculated by converting Eq. (2) to an integral over the spatial variation:

$$I_{dc}(V_{dc}) = \sum_{n=-\infty}^{\infty} L^{-1} \times \int_0^L J_n^2[eV_{rf}(X)/hf]dX I_0(V_{dc}+nhf/e). \quad (5)$$

$V_{rf}(X)$ is given by[15]

$$V_{rf}(X) = V_{rf0}[(1+\rho)^2 - 4\rho \sin^2(\pi X/L)]^{1/2}, \quad (6)$$

where L is the width of the junction and the reflection coefficient ρ is given by $\rho = (\text{VSWR}-1)/(\text{VSWR}+1)$.

The solid lines in Figs. 4 are calculated from Eqs. (5) and (6) using a VSWR of 5. As expected, the effect of the integration in Eq. (5) is a smoothing of the Bessel-function curve, and for any VSWR greater than 1 has the effect of removing the zeros from the V_{rf} dependence. The exact form of our calculated curve depends on the assumed VSWR but is not sensitive to the number of wavelengths in the standing-wave pattern. Experimentally the VSWR is very difficult to determine, and thus we are primarily concerned with qualitative agreement. With this in mind, it is clear

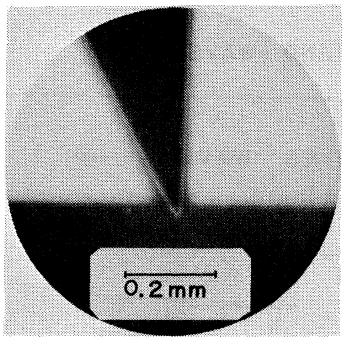

FIG. 6. Photograph of a very small overlap junction.

that the general form of Eq. (5) is in agreement with the data. Although our results are shown only for orders 0, 1, and 2, by using derivative techniques we have observed similar agreement up to the 11th order.

A similar analysis can be applied to the rf-induced steps arising from the ac Josephson effect. When the J_n dependence of the ac Josephson steps in Eq. (3) is integrated over the spatial variation of Eq. (6), the result is again a smoothing of the curve with the disappearance of the periodic zeros. In contrast to the quasiparticle steps, the ac Josephson steps are constant voltage and thus have a sharply defined height in a I-V curve. Unfortunately, as the I-V curve is traced out, it is not possible to know whether a step attained its maximum value before the current switched to the background curve. In spite of this difficulty, measurements of the ac Josephson steps from the same set of I-V curves used to plot the data of Figs. 4 show their V_{rf} dependence to be consistent with the standing-wave model. With increasing rf voltage, the steps appear in order, varying in magnitude but definitely not showing the periodic oscillation indicated in Eq. (3). Further, the order of appearance of both the quasiparticle steps and the Josephson steps is consistent with the same value of V_{rf}; i.e., we always observe about twice as many Josephson steps as quasiparticle steps. This is a result of the factor-of-2 difference in the arguments of $|J_n|$ for the Josephson steps and J_n^2 for the quasiparticle steps.

C. Small-Junction Experiments

If similar measurements are made on a junction which is not large enough to support a standing-wave pattern, then Eq. (2) should correctly describe the V_{rf} dependence of the quasiparticle steps. We have performed such an experiment on a very small junction at 20 GHz ($hf/e=0.083$ mV) and found this prediction to be correct. This small junction was made using an in-line geometry where a sharp point of evaporated material just barely overlaps the edge of the second thin film. The oxide barrier was prepared as before. Figure 6 is a photograph of the junction used in this experiment.

A lower frequency, 20 GHz, was used to improve the uniformity of V_{rf} across the junction. Since this frequency is near the limit of resolution of the quasiparticle steps, it was necessary to use derivative techniques to measure the V_{rf} dependence of the various steps. Portions of these derivative curves (dI/dV versus V) at six different values of V_{rf} are reproduced in Fig. 7. The scale divisions indicate the voltages at which the steps appear and the V_{rf} values are estimated by comparison with Eq. (2). Thus, with $V_{rf}=0$, we see only the $n=0$ step, which is represented by the large peak in conductance at the gap voltage, $V=2\Delta/e=1.17$ mV. For $V_{rf}=0.105$ mV, the $n=0$ step has decreased and the $n=1$ step is coming to a maximum. At $V_{rf}=0.166$ mV, the conductance peak for the $n=0$

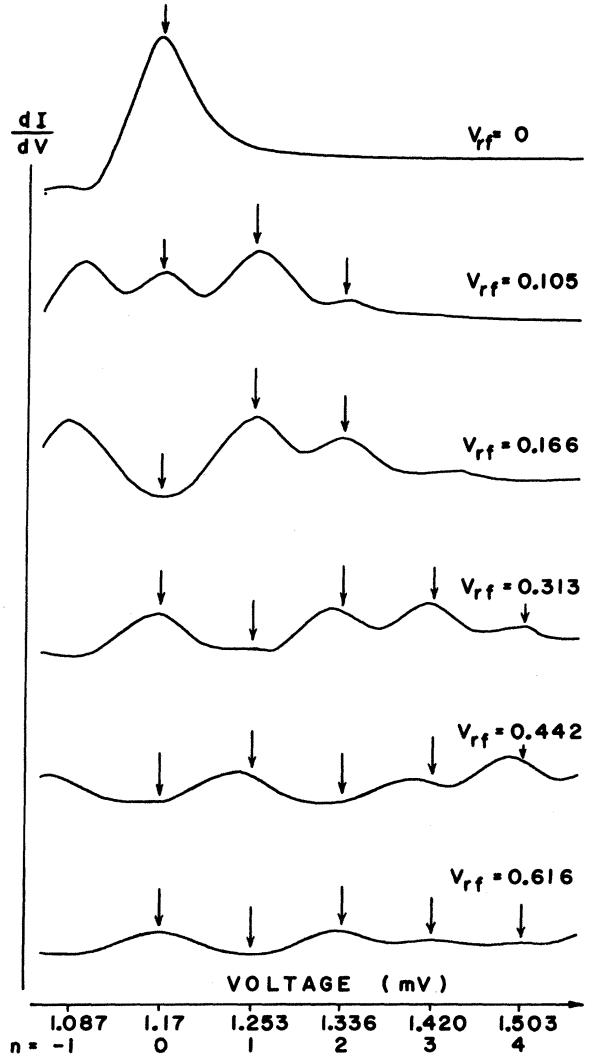

FIG. 7. Portions of the derivative curves dI/dV versus V for six different values of V_{rf}. The arrows indicate the positions of the quasiparticle steps.

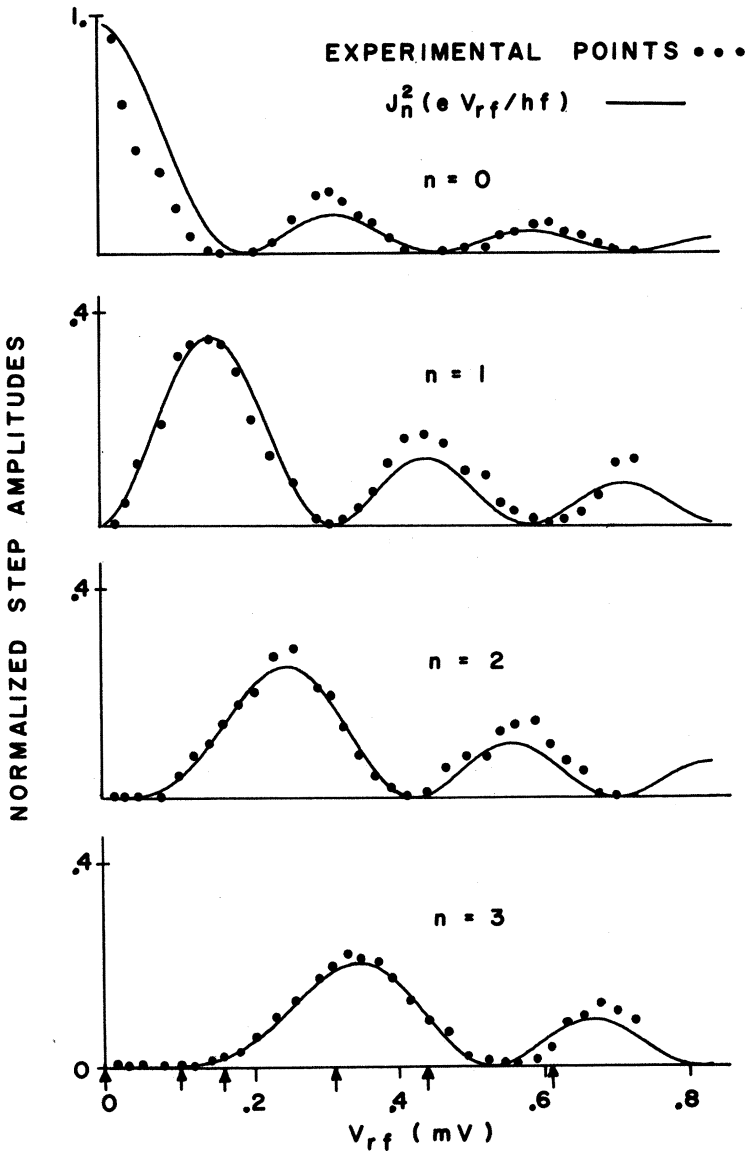

FIG. 8. Quasiparticle-step amplitudes for the $n=0$, 1, 2, and 3 steps as a function of V_{rf}. The data points are for the very small junction of Fig. 6.

step is missing and the $n=1$ step has reached a maximum.

In order to compare this behavior directly with Eq. (2), we have estimated the magnitude of the conductance peaks and fitted these data to the J_n^2 curves using the same procedure as for Figs. 4. The results for the $n=0$, 1, 2, and 3 steps are shown in Fig. 8. The arrows on the V_{rf} axis correspond to the derivative curves of Fig. 7. In view of the measuring procedure the agreement is excellent. In particular, the positions of the maxima and zeros agree well with the theory.

This same junction was also exposed to 80-GHz radiation. At this higher frequency the behavior of the quasiparticle steps was similar to Figs. 4, indicating the existence of standing-wave variations.

A similar result has been obtained by Longacre and Shapiro[16] from experiments on point-contact junctions. Their data at 73 GHz show the V_{rf} dependence of both the ac Josephson and the quasiparticle steps to be consistent with Eqs. (2) and (3). The small area inherent in point-contact junctions permits the use of very high frequencies without exciting standing-wave modes.

D. Summary

We have found, in common with prior work, that experiments at high frequencies with conventional tunnel junctions yield results for the rf-voltage dependence of photon-assisted tunneling steps that disagree with theoretical predictions. These discrepancies vanish when the theory is modified to take into account the stand-

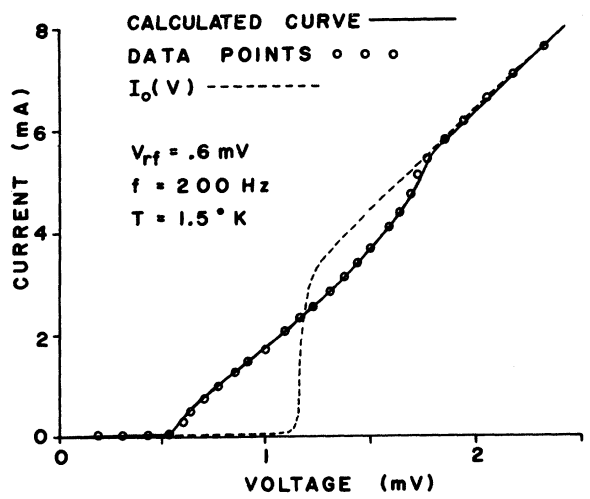

Fig. 9. *I-V* curves with and without an applied rf field at 200 Hz.

ing-wave rf-voltage variations which exist in these junctions for high frequencies. To avoid such standing waves, we have carried out a similar experiment with a very small area junction and have found excellent agreement with the unmodified theory.

IV. CLASSICAL rf DETECTION

In this section we consider the relationship between experimental and theoretical values of V_{rf}. Since, in general, it is not possible to measure V_{rf} in a microwave experiment, values of V_{rf} have been determined by fitting experimental results to a theoretical expression such as Eq. (2). In the previous work,[3,6,8] this led to values of V_{rf} which were from one to two orders of magnitude greater than the value of V_{rf} calculated from the known microwave field in the vicinity of the junction. In these experiments the junction was located in a microwave cavity. Our experiments place the junction across a terminated waveguide. In either case, Werthamer[1] has pointed out that the rf voltage across the junction cannot accurately be estimated by taking the rf voltage across an equivalent section of waveguide or cavity. The existence of standing waves in the junction supports this conclusion and suggests that the rf voltage across the junction may actually be considerably greater than previously estimated.

Further support for the theory can be gained by examining Eq. (2) at low frequencies ($hf/e<60$ μV) where the original *I-V* curve is smooth with respect to voltage increments of hf/e. For most superconducting tunnel junctions this means anything less than about 15 GHz. For these frequencies the individual step structure is not resolved and the detailed V_{rf} dependence of individual steps cannot be studied. Instead, the *I-V* curves show a gradual smoothing as rf power is applied. For this case we now demonstrate that Eq. (2) reduces to the equation of classical rf detection.

Letting $\alpha=eV_{rf}/hf$, the assumption of low frequency implies that α is large and Eq. (2) may thus be written in integral form:

$$I_{dc}(V_{dc})=\int_{-\infty}^{\infty} J_\eta^2(\alpha)I_0(V_{dc}+\eta V_{rf}/\alpha)\,d\eta. \quad (7)$$

Since the value of $J_\eta^2(\alpha)$ decreases very rapidly for $\eta>\alpha$, the limits of integration may be changed to $\pm\alpha$. Also, for large values of α, Eq. (7) is not sensitive to the oscillations of $J_\eta^2(\alpha)$, but rather to the average value of $J_\eta^2(\alpha)$ over a small range of η. We define this average value as

$$\langle J_\eta^2(\alpha)\rangle_{av}=\int_{\eta-\Delta\eta}^{\eta+\Delta\eta} J_\eta^2(\alpha)\,d\eta, \qquad 1<\Delta\eta\ll\alpha. \quad (8)$$

With these two approximations Eq. (7) becomes

$$I_{dc}(V_{dc})=\int_{-\alpha}^{\alpha}\langle J_\eta^2(\alpha)\rangle_{av}I_0(V_{dc}+\eta V_{rf}/\alpha)\,d\eta. \quad (9)$$

Using standard asymptotic approximations[17] for $J_\eta^2(\alpha)$ over the relevant ranges of η and α, it is easily shown that

$$\langle J_\eta^2(\alpha)\rangle_{av}=(\pi\alpha)^{-1}[1-(\eta/\alpha)^2]^{-1/2}. \quad (10)$$

Let $\beta=\eta/\alpha$ and substitute (10) into (9):

$$I_{dc}(V_{dc})=\pi^{-1}\int_{-1}^{+1}(1-\beta^2)^{-1/2}I_0(V_{dc}+V_{rf}\beta)\,d\beta. \quad (11)$$

Make the change of variable

$$d\theta=(1-\beta^2)^{-1/2}\,d\beta,$$

which implies that $\beta=\sin\theta$, and Eq. (11) becomes

$$I_{dc}(V_{dc})=\pi^{-1}\int_{-\pi/2}^{\pi/2} I_0(V_{dc}+V_{rf}\sin\theta)\,d\theta. \quad (12)$$

This is the equation of classical rf detection. Computer studies comparing Eqs. (2) and (12) have shown agreement to better than 1% for all α when the frequency is 5 GHz and I_0 is a typical experimental *I-V* curve. The agreement improves rapidly as frequency decreases.

This analysis is significant because it shows the theory to be correct in the limit of low frequency. To further demonstrate this point we performed an experiment at 200 Hz where the value of V_{rf} could be directly measured. The 200-Hz "rf" was applied to the junction leads and V_{rf} measured directly on a scope. For this experiment a 0.01-Ω shunt across the junction provided an essentially constant-voltage drive. The dc *I-V* curve was plotted on an *X-Y* recorder with a 2-Hz bandwidth. With V_{rf} set at 0.6 mV we adjusted the dc bias to obtain a series of points. Figure 9 shows the theoretical curve for $V_{rf}=0.6$ mV and our experimental points. The base curve $I_0(V)$ is also shown for clarity. The excellent agreement is expected.

The fact that Eq. (2) has been shown to be correct in the limit of low frequency gives further support to our contention that the V_{rf} dependence of Eq. (2) is

correct at all frequencies. The reported discrepancies of one or two orders of magnitude between experimental and theoretical V_{rf} values must be attributed to the procedures used in estimating V_{rf}.

V. SUMMARY AND CONCLUSIONS

In this section we summarize our results and comment on other contributions in the field. We have presented four main points: (a) A standing-wave model is proposed as a modification of the existing theory in order to explain the V_{rf} dependence of the photon-assisted tunneling steps. (b) Simultaneous measurements of both the ac Josephson steps and the quasiparticle steps for the same junction are consistent with this standing-wave model. (c) In very small junctions with no spatial variation of the rf voltage, the V_{rf} dependence of the quasiparticle steps is in excellent agreement with the original theory. (d) The theory of the quasiparticle steps reduces exactly to classical rf detection in the limit of low frequency.

Cook and Everett[6] were the first to report in detail on the V_{rf} dependence of the step-current amplitudes in photon-assisted tunneling. Their data parallel ours in that the step currents did not follow the theoretical J_n^2 dependence. To explain this result they have made a modification of the theory which in effect makes the location of the zero of potential an important physical parameter. Their analysis leads to a V_{rf} dependence qualitatively similar to our standing-wave result and thus is in reasonable agreement with experiment. We reject their argument for three reasons. First, it cannot explain the J_n^2 dependence we observe in very small junctions. Second, their result does not reduce to classical rf detection for low frequencies, and finally Büttner and Gerlach[11] have shown that by properly symmetrizing the analysis the result is independent of the zero of potential.

In a recent paper, Teller and Kofoed[7] have reported excellent agreement with the Cook-Everett analysis. Again, we believe that this agreement is fortuitous and we suggest a comparison of these data with Eq. (5).

Sweet and Rochlin[8] have carried out low-frequency experiments with tin-oxide-tin junctions at 3.9 GHz. By fitting V_{rf} at one point, they obtained excellent agreement with Eq. (2). In this frequency range, Eqs. (2) and (12) are the same and such excellent agreement is to be expected. This experiment is not fundamentally different from our experiment at 200 Hz except that in our case a measured V_{rf} was used. They also criticize the applicability of Eq. (3) to their data for the zero-voltage Josephson current because the V_{rf} required to fit the first zero from Eq. (3) ($n=0$) correlates poorly with the V_{rf} required to fit their I-V curves to Eq. (2). To rely thus on one datum as an important test of the theory is clearly hazardous, especially in view of the well-known susceptibility of the zero-voltage current to microshorts. Our data, as well as those of Longacre and Shapiro,[16] include the behavior of many steps, rather than just the $n=0$ step, and strongly indicate the validity of Eq. (3) as well as its proper correlation with Eq. (2).

Finally, we are led by all the evidence to conclude that Werthamer's theory of rf-induced effects in superconducting tunnel junctions is on very firm experimental ground provided the theory is extended to include, where appropriate, the effects of spatial rf-voltage variation.

---

* Work supported by the National Science Foundation under Grant No. GK-10562.

[1] N. R. Werthamer, Phys. Rev. **147,** 255 (1966).
[2] A. H. Dayem and R. J. Martin, Phys. Rev. Letters **8,** 246 (1962).
[3] P. K. Tien and J. P. Gordon, Phys. Rev. **129,** 647 (1963).
[4] C. C. Grimes and Sidney Shapiro, Phys. Rev. **169,** 397 (1968).
[5] S. Shapiro, A. R. Janus, and S. Holly, Rev. Mod. Phys. **36,** 223 (1964).
[6] C. F. Cook and G. E. Everett, Phys. Rev. **159,** 374 (1967).
[7] S. Teller and B. Kofoed, Solid State Commun. **8,** 235 (1970).
[8] J. N. Sweet and G. I. Rochlin, Phys. Rev. B **2,** 656 (1970).
[9] S. Shapiro and A. R. Janus, in *Proceedings of the Eighth International Conference on Low-Temperature Physics, London, 1962,* edited by R. O. Davies (Butterworths, London, 1963), p. 321.
[10] R. J. Pederson and F. L. Vernon, Jr., Appl. Phys. Letters **10,** 29 (1967).
[11] H. Büttner and E. Gerlach, Phys. Letters **27A,** 226 (1968).
[12] S. Shapiro, Phys. Rev. Letters **11,** 80 (1963).
[13] J. C. Swihart, J. Appl. Phys. **32,** 461 (1961).
[14] D. D. Coon and M. D. Fiske, Phys. Rev. **138,** A471 (1965).
[15] R. E. Collin, *Foundations for Microwave Engineering* (McGraw-Hill, New York, 1966), pp. 90–91.
[16] A. Longacre, Jr., and Sidney Shapiro (unpublished).
[17] *Handbook of Mathematical Functions,* edited by M. Abramowitz and I. Stegun (Dover, New York, 1965), Eqs. 9.2.1 and 9.3.3.

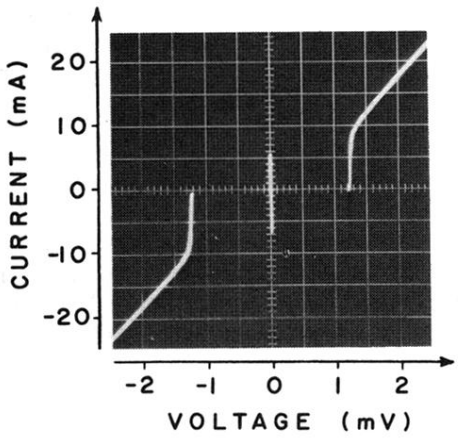

FIG. 1. Oscilloscope trace of the I-V curve for a typical 0.1-Ω superconducting tin-oxide-tin junction.

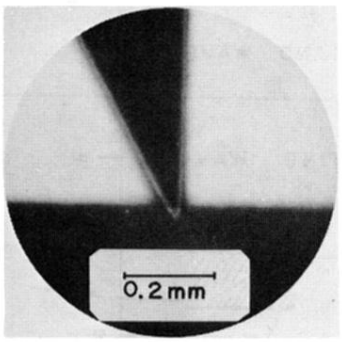

FIG. 6. Photograph of a very small overlap junction.